symmetry

MDPI

Article

Directed Evolution of a Glutathione Transferase for the Development of a Biosensor for Alachlor Determination

Fereniki Perperopoulou [1], Maria Fragoulaki [1], Anastassios C. Papageorgiou [2,3] and Nikolaos E. Labrou [1,*]

[1] Laboratory of Enzyme Technology, Department of Biotechnology, School of Applied Biology and Biotechnology, Agricultural University of Athens, GR-11855 Athens, Greece; perperopoulouf@aua.gr (F.P.); mfrag@gmail.com (M.F.)
[2] Turku Bioscience Centre, University of Turku, 20521 Turku, Finland; anapap@utu.fi
[3] Turku Bioscience Centre, Åbo Akademi University, 20521 Turku, Finland
* Correspondence: lambrou@aua.gr

Abstract: In the present work, DNA recombination of three homologous tau class glutathione transferases (GSTUs) allowed the creation of a library of tau class *Gm*GSTUs. The library was activity screened for the identification of glutathione transferase (GST) variants with enhanced catalytic activity towards the herbicide alachlor (2-chloro-2′,6′-diethyl-N-(methoxymethyl)acetanilide). One enzyme variant (*Gm*GSTsf) with improved catalytic activity and binding affinity for alachlor was identified and explored for the development of an optical biosensor for alachlor determination. Kinetics analysis and molecular modeling studies revealed a key mutation (Ile69Val) at the subunit interface (helix α3) that appeared to be responsible for the altered catalytic properties. The enzyme was immobilized directly on polyvinylidenefluoride membrane by crosslinking with glutaraldehyde and was placed on the inner surface of a plastic cuvette. The rate of pH changes observed as a result of the enzyme reaction was followed optometrically using a pH indicator. A calibration curve indicated that the linear concentration range for alachlor was 30–300 μM. The approach used in the present study can provide tools for the generation of novel enzymes for eco-efficient and environment-friendly analytical technologies. In addition, the outcome of this study gives an example for harnessing protein symmetry for enzyme design.

Keywords: alachlor; glutathione transferase; herbicides; protein engineering; biosensor; pesticides

Citation: Perperopoulou, F.; Fragoulaki, M.; Papageorgiou, A.C.; Labrou, N.E. Directed Evolution of a Glutathione Transferase for the Development of a Biosensor for Alachlor Determination. *Symmetry* **2021**, *13*, 461. https://doi.org/10.3390/sym13030461

Academic Editor: Christophe Humbert

Received: 19 February 2021
Accepted: 5 March 2021
Published: 12 March 2021

1. Introduction

Glutathione transferases (GSTs; EC. 2.5.1.18) are a widely spread family of enzymes found in both eukaryotes and prokaryotes [1,2]. They catalyze the conjugation of glutathione (GSH) with a range of hydrophobic xenobiotic compounds such as drugs, environmental pollutants, and pesticides, including chloroacetanilide herbicides [3–9]. Their catalytic versatility and wide-substrate specificity stem from their structural flexibility and active-site plasticity [3,10–13]. They are homodimers or heterodimers. The isoenzyme *Gm*GST4-4 from *Glycine max* is a homodimer protein with an open V-shaped configuration with 2200 Å^2 of the accessible surface buried at the interface, smaller than that of most other classes of GSTs (2800–3400 Å^2). Each subunit has two domains, a small α/β domain, at the N-terminus, and a large β-helical domain, at the C-terminus. The former hosts the GSH-binding site (G-site) on top of the α/β domain [3,14,15]. A hydrophobic pocket (H-site) overlaps the two domains and binds the hydrophobic substrates.

The ability of GSTs to conjugate GSH with xenobiotics has been exploited for the development of enzyme-based biosensors for the determination and monitoring of such compounds in biological and environmental samples [16–22]. A range of different GST isoenzymes has been used so far for the fabrication of optical, electrochemical or potentiometric biosensors for measuring pesticides, such as the herbicide atrazine [16], the insecticides DDT [17], malathion [18], dieldrin and spiromesifen [19], α-endosulfan [20],

and molinate [21]. In addition, a GST-based biosensor has been developed for the determination of anticancer drugs [23].

Pesticides, although they are useful agricultural agents for fighting pests and can certainly increase food production, are also harmful to human health and environment [24–26]. Regulatory requirements have posed strict restrictions on maximum residue levels (MRL) that must be met before food products can enter a market [27–29]. As a consequence, there is a need for a robust analytical methods suitable for pesticides determination with high accuracy in food and environmental samples.

In vitro directed evolution is regarded as the most efficient method for expanding sequence diversity and creating enzymes with improved or novel properties [29,30]. Increasingly, directed evolution has been applied to create enzymes catalyzing reactions either in a more efficient way or reactions that have not been observed in nature by taking advance of the promiscuous nature of enzymes [30]. A range of different methods and techniques have been developed that have enabled the evolution of any protein [29,30], pathway [31], network [32], or entire organism of interest [33].

In the present work, a library of tau class GSTs was created using DNA shuffling. The library was activity screened, allowing the selection of an engineered enzyme (*Gm*GSTsf) with high conjugating activity towards the herbicide alachlor. The selected enzyme was characterized, immobilized on polyvinylidenefluoride membrane, and was used for the construction of an optic biosensor for alachlor determination in water samples. Alachlor displays high toxicity to humans and animals [34,35]. Due to its extensive application in agriculture, contamination of food, water, and air has become significant and, as a consequence, adverse health effects affect all organisms [34,35].

2. Materials and Methods

2.1. Materials

Reduced GSH, 1-chloro-2,4-dinitrobenzene (CDNB), antibiotics, and all other enzyme substrates were obtained from Sigma-Aldrich (St. Louis, MO, USA). Miniplasmid isolation kit was purchased from Macherey–Nagel (Kirkel, Germany) and QIAquickTM Gel Extraction kit from Quiagen. The pesticides were purchased from Riedel de Haen (Hanover, Germany).

2.2. Methods

2.2.1. Library Construction

Three isoenzymes from *Glycine max* (*Gm*GSTU2-2, *Gm*GSTU4-4, and *Gm*GSTU10-10) [36–38] were used as parent sequences for directed evolution using the DNA shuffling method [39]. Shuffled library was constructed as described by Axarli et al. (2016) [40].

Expression, Purification, and Screening of the Wild-Type and Mutant Enzymes

*Gm*GSTUs were expressed in *Escherichia coli* M15 [pREP4] and purified by affinity chromatography as described by Axarli et al. (2008) [38]. Protein purity was judged by PAGE. For activity screening of the shuffled library, transformants were grown at 37 °C in LB medium (10 mL), and the GSH/alachlor conjugation activity in crude cell free extracts was measured as described by Skopelitou and Labrou (2010) [41].

2.2.2. Assay of Enzyme Activity and Kinetic Analysis

Enzyme assays and steady-state kinetic measurements using CDNB and GSH were performed according to published methods [40]. Initial velocities were determined in the presence of a fixed concentration of GSH (2.5 mM) and variable concentrations of CDNB (0.015–0.150 mM). Alternatively, CDNB was used at a fixed concentration (1.5 mM) and the GSH was varied (0.05–0.5 mM). The steady-state data were analyzed by non-linear regression analysis using the GraphPad Prism Software (Version 5.03).

2.2.3. Molecular Modeling

The structure of the engineered *Gm*GSTU with high activity towards alachlor (*Gm*GSTsf) was predicted using homology modeling (SWISS-MODEL) based on the structure of the parent enzyme *Gm*GSTU4-4 (PDB code 2vo4), determined at 1.75 Å resolution [38]. The sequence identity between the two enzymes is 95.4%, allowing the construction of a reliable model. The reliability and quality of the model was evaluated using GMQE score (0.84) [42]. The global and per-residue model quality was assessed using the QMEAN (Z-score 0.9) scoring function [43]. Moreover, PROCHECK [44] was employed to further evaluate the quality of the modelled GST. Verify3D [45] was also used to evaluate whether the model has a similar fold to known protein structures. The program PyMOL (http://www.pymol.org/) was employed for the visualization of the protein structures. Non-covalent interactions were analyzed using the Protein Contacts Atlas [46] and Arpeggio server [47].

2.2.4. Immobilization of Enzyme and Assessment of Enzyme Activity

Immobilization of *Gm*GSTsf was achieved using glutaraldehyde chemistry and deposition on a polyvinylidenefluoride membrane (Durapole). The procedure was performed as follows: a polyvinylidenefluoride membrane was immersed and incubated for 30 min in potassium phosphate buffer (50 mM, pH 8.5). Bovine serum albumin (5 mg) was dissolved in potassium phosphate buffer (50 mM, pH 8.5) containing enzyme (5 U, previously dialyzed against 50 mM potassium phosphate buffer, pH 8.5). Glutaraldehyde solution was added to the mixture (final concentration 8% v/v), stirred for 15 s, and deposited on the surface of the polyvinylidenefluoride membrane. The membrane was incubated at 4 °C for 45 min and then rinsed three times with potassium phosphate buffer (50 mM, pH 7.5) to remove unreacted compounds and reaction byproducts. The same procedure was also carried out for the preparation of enzyme-free membranes (control). The membrane-immobilized enzyme was placed on the inner surface of a plastic cuvette (4 mL).

Assessment of the activity of the immobilized *Gm*GSTsf enzyme was carried out using the CDNB/GSH or the alachlor/GSH substrate system. The enzyme reaction (37 °C) was monitored using a pH electrode. The composition of the reaction was: potassium phosphate buffer (1 mM, 10 mM NaCl pH 6.5) containing 0.5 mM CDNB or 0.5 mM alachlor (dissolved in acetone), 1 mM GSH, and 0.5 units of enzyme. Alternatively, the reaction was carried out in potassium phosphate buffer (3 mL, 50 mM, pH 6.5), containing 2.5 mM GSH, 1 mM CDNB, and immobilized enzyme. The mixture was incubated at 37 °C. The progress of the reaction was followed by measuring the absorbance at 340 nm. The enzyme-free membrane was used as a control.

Steady-state kinetics analysis of the membrane-immobilized *Gm*GSTsf was carried out using the CDNB/GSH substrate system in potassium phosphate buffer (0.1 M, pH 6.5). The assay mixture contained 2.5 mM GSH and variable CDNB concentrations (0.05 mM–1.0 mM). The reactions were carried out at 37 °C for 30 min. Samples were taken at 5 min intervals for measuring the absorbance at 340 nm.

2.2.5. Stability Analysis of the Free and Immobilized Enzyme

The stability upon storage of the free and membrane-immobilized *Gm*GSTsf enzyme was studied at 4 °C in potassium phosphate buffer (1 mM potassium phosphate buffer, 10 mM NaCl, pH 7.5). Enzyme inactivation was followed by assaying the enzyme activity using the CDNB/GSH substrate system.

2.2.6. Colorimetric Assays for the GST-Catalyzed Alachlor Conjugation Reaction

The membrane-immobilized enzyme was placed on the inner surface of a plastic cuvette (4 mL). The GST-catalyzed alachlor conjugation reaction was monitored in potassium phosphate buffer (3 mL, 1 mM potassium phosphate buffer, 10 mM NaCl, pH 7.5) containing 2.5 mM GSH, 0.05 mM bromocresol green, and alachlor (0 mM to 0.3 mM). The reactions were incubated at 37 °C and spectra (300 to 750 nm) were recorded at time intervals (0, 10, 20 and 30 min). The absorbance change at 620 nm versus time was used for

measuring enzyme activity for each alachlor concentration. The slope of each graph was used for the construction of a calibration curve (slope versus alachlor concentration).

2.2.7. Determination of Alachlor in Natural Water Samples

Recovery experiments were achieved using natural tap water samples (collected from Athens water supply network), spiked with known concentrations of alachlor (0.02 mM, 0.04 mM, 0.08 mM, and 0.17 mM). A sample of zero alachlor concentration water was used as a control. The concentrations of spiked alachlor were calculated based on a calibration curve obtained as described above.

3. Results and Discussion

3.1. Screening of GmGSTUs Library for Identifying a Shuffled Enzyme for the Development of a Biosensor for Alachlor Determination

The isoenzymes *Gm*GSTU2-2, *Gm*GSTU4-4, and *Gm*GSTU10-10 from *Glycine max* share 88–91% sequence identity; however, their specificity towards different electrophile xenobiotics varies significantly. Worthy of note, the specific activity of the three *Gm*GSTUs for the herbicides atrazine or alachlor ranges between 0 to 0.76 nmol/min × mg and 8 to 166 nmol/min × mg, respectively [48,49]. Therefore, the natural catalytic promiscuity of the *Gm*GSTUs provides a promising starting point for the development of engineering *Gm*GSTU variants with engineered activity and/or specificity towards the pesticide alachlor.

The three isoenzymes *Gm*GSTU2-2, *Gm*GSTU4-4, and *Gm*GSTU10-10 were used as parent sequences for directed evolution using the DNA shuffling method [39,40]. The *Gm*GSTUs library was activity screened for the isolation of enzyme variants with improved catalytic activity towards the herbicide alachlor. One enzyme variant (*Gm*GSTsf) that displayed the highest specific activity (Figure 1) was identified and selected for further characterization. This variant was sequenced (Figure 2) and showed that it has been derived from *Gm*GSTU4-4 with segments mainly from *Gm*GSTU2-2 and a few from *Gm*GSTU10-10. The sequence of *Gm*GSTsf possesses eight mutations (see Table 1), a three amino acid deletion, and two-point mutations compared to the parent *Gm*GSTU4-4 enzymes (Figure 2). The *Gm*GSTsf variant was expressed in *E. coli*, purified and subjected to steady-state kinetic analysis (Table 2). The results confirmed that the enzyme displays improved k_{cat} value towards alachlor and CDNB, the common substrate for assaying GSTs. Although the enzyme showed slightly increased K_m value for both electrophile substrates, its specificity constants (k_{cat}/K_m) appeared augmented for both substrates, suggesting that the engineered *Gm*GSTsf enzyme exhibits improved specificity towards CDNB and alachlor compared to the parent enzyme *Gm*GSTU4-4.

Table 1. Summary of mutations and deletions found in *Gm*GSTsf sequence (a derivative of *Gm*GSTU4-4), in comparison with the parent enzymes *Gm*GSTU2-2 and *Gm*GSTU10-10. The other amino acid sequence is identical to that of *Gm*GSTU4-4. Numbering refers to the parent enzyme *Gm*GSTU4-4.

***Gm*GSTsf (Amino Acid Replacement in *Gm*GSTU4-4 Sequence)**	**Source of Mutations**
Ser2Gln	Spontaneous mutation
Glu4Gln	Spontaneous mutation
Tyr32Ser	*Gm*GSTU2-2
Ile69Val	*Gm*GSTU2-2
Asn149Asp	*Gm*GSTU2-2
Val158Ile	*Gm*GSTU2-2
Tyr161Asp	*Gm*GSTU2-2
Deletion (166AlaTyrGlu168)	*Gm*GSTU2-2
Thr172Ser	*Gm*GSTU2-2 or *Gm*GSTU10-10
Ile183Val	*Gm*GSTU2-2 or *Gm*GSTU10-10
Met210Val	*Gm*GSTU10-10

Table 2. Steady-state kinetic analysis of the *Gm*GSTU4-4 and *Gm*GSTsf using 1-chloro-2,4-dinitrobenzene (CDNB) and alachlor as electrophile substrates.

Enzyme	k_{cat} (min^{-1})	K_m (μM)(GSH)	K_m (μM)(CDNB)	k_{cat}/K_m(GSH) ($min^{-1}\mu M^{-1}$)	k_{cat}/K_m(CDNB) ($min^{-1}\mu M^{-1}$)
GSH/CDNB					
*Gm*GSTU4-4 [1]	149 ± 18.6	159 ± 18.9	158 ± 31.6	0.9	0.9
*Gm*GSTsf	472 ± 42.6	223 ± 23.3	351 ± 48.1	2.1	1.3
Enzyme	**k_{cat} (min^{-1})**	**K_m (μM)(GSH)**	**K_m (μM)(Alachlor)**	**k_{cat}/K_m(GSH) ($min^{-1}\mu M^{-1}$)**	**k_{cat}/K_m(CDNB) ($min^{-1}\mu M^{-1}$)**
GSH/Alachlor					
*Gm*GSTU4-4	4.5	210	225	0.021	0.020
*Gm*GSTsf	15.2	319	352	0.047	0.043

[1] The data for *Gm*GSTU4-4 were reported by Axarli et al., (2008) [38] and included for comparison.

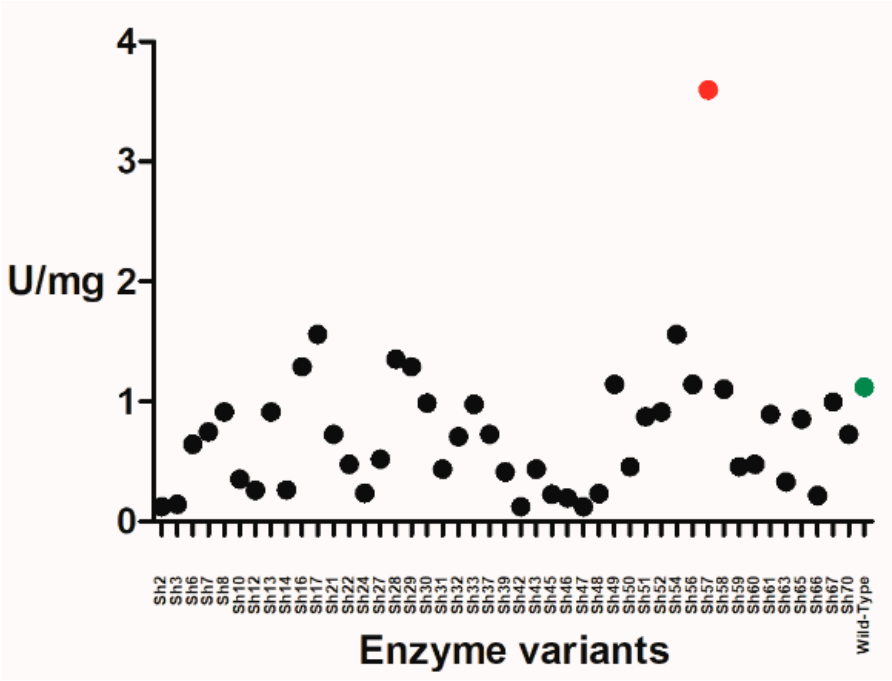

Figure 1. Activity screening of the tau class glutathione transferases (*Gm*GSTUs) library towards alachlor. Green filled circle: the wild type *Gm*GSTU4-4; Black filled circle: members of the library (Sh). Red-filled circle: the enzyme variant with the highest activity.

Kinetic inhibition constant (K_i) and half-maximal inhibitory concentration (IC_{50}) were also measured to evaluate the effect of mutations on the affinity of the enzyme for alachlor. Since alachlor is a substrate for the enzyme, the inactive hydrolyzed analogue (non-substrate) of alachlor (hAlachlor; 2-hydroxyl-2′,6′-diethyl-N-(methoxymethyl)acetanilide), was employed in the study and the results are shown in Figure 3 and listed in Table 3. The determination of K_i and IC_{50} values for the *Gm*GSTU4-4 and *Gm*GSTsf variants provides a direct estimation of the binding affinity of hAlachlor towards the enzyme. The analysis showed that the *Gm*GSTsf variant displayed about 17-fold lower K_i and 4-fold lower IC_{50} values compared to the parent enzyme *Gm*GSTU4-4, suggesting that the affinity of the variant has been improved significantly.

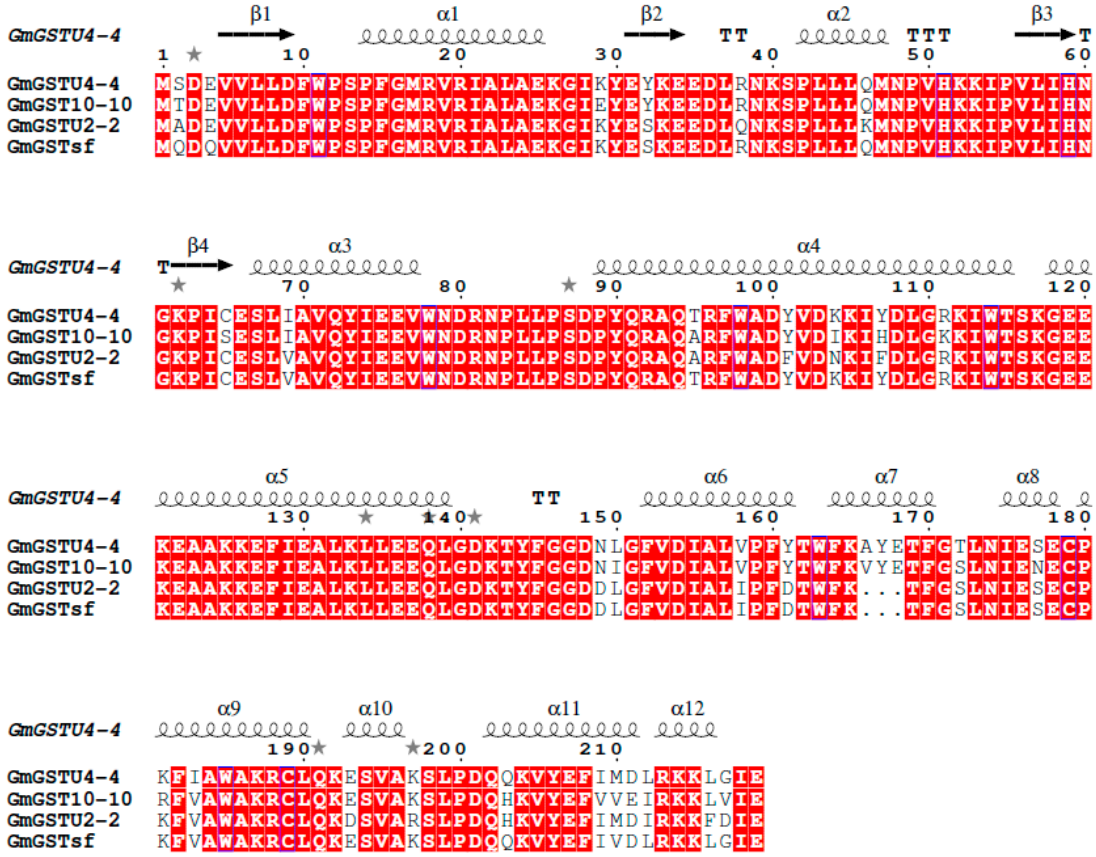

Figure 2. Alignments of the parent sequences *Gm*GSTU2-2, *Gm*GSTU4-4 and *Gm*GSTU10-10 with the sequence of the *Gm*GSTsf enzyme. The secondary structure of *Gm*GSTU4-4 (PDB code 2vo4) is shown at the top. The figure was produced using ESPript [50]. *Gm*GSTU4-4 numbering and secondary structure (helices and arrows) are shown above the alignment. Beta turns are marked with TT. Conserved areas are shown shaded. The symbol (○) above sequences indicates important amino acid residues. NCBI accession numbers for sequences are in parentheses: *Gm*GSTU4-4 (AAC18566), *Gm*GSTU2-2 (CAA71784), and *Gm*GSTU10-10 (AAG34800.1).

Table 3. Kinetic inhibition constant (K_i) and half maximal inhibitory concentration (IC_{50}) of hAlachlor towards the *Gm*GSTU4-4 and *Gm*GSTsf enzymes.

Enzyme	K_i (μM)	IC_{50} (μM)
*Gm*GSTU4-4	127.3 ± 12	65.8 ± 11.8
*Gm*GSTsf	7.5 ± 0.9	17.5 ± 5.2

3.2. Molecular Modeling

Homology modeling was employed to predict the structure of the *Gm*GSTsf variant and put the results of the kinetic analysis in a structural context. Figure 4a shows the position of amino acid residues that have been mutated during the DNA shuffling protocol in the *Gm*GSTsf variant. Most of the mutated amino acids are located at regions that appear to be insignificant in terms of catalysis or binding affinity, because they are distant from the active site and are exposed to the solvent without participating, directly or indirectly, in key molecular interactions. The only exception is the Ile69Val mutation, which seems to have a profound effect on the structure and catalysis. The amino acid at position 69 is located in the short helix α3 (residues 66–78), to which previous studies have attributed important functional roles in substrate binding and catalysis. Helix α3 provides two key amino acid residues, Glu66 and Ser67, that directly participate in GSH binding. In particular, the side chain of Glu66 forms a strong ionic interaction with the amino group of glutamyl residue of GSH. The side chain of Ser67 is hydrogen bonded with γ-carboxylate group of

GSH. Moreover, the side chains of Glu66 and Ser67 are involved in the formation of the electron-sharing network, a key determinant in the catalytic mechanism of *Gm*GSTU4-4 [49] and other GSTs [51]. In the *Gm*GSTU4-4, the total number of non-covalent interactions that Ile69 makes are significantly larger, compared to that of Val69 in the *Gm*GSTsf variant (Table 4). Therefore, the Ile69Val mutation seems to affect the structural integrity of helix α3, causing, as a consequence, structural rearrangements to Glu66 and Ser67.

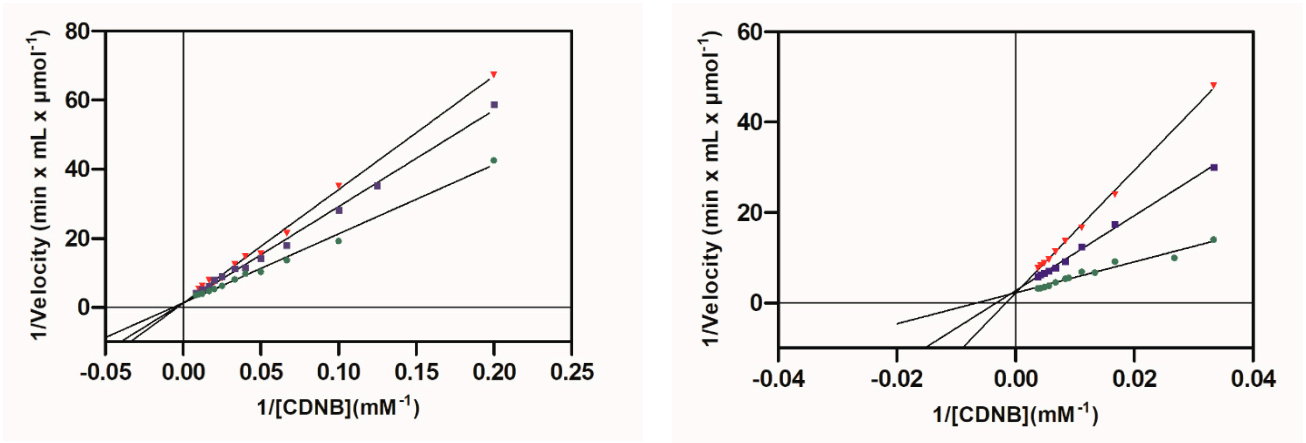

(**a**) (i) (ii)

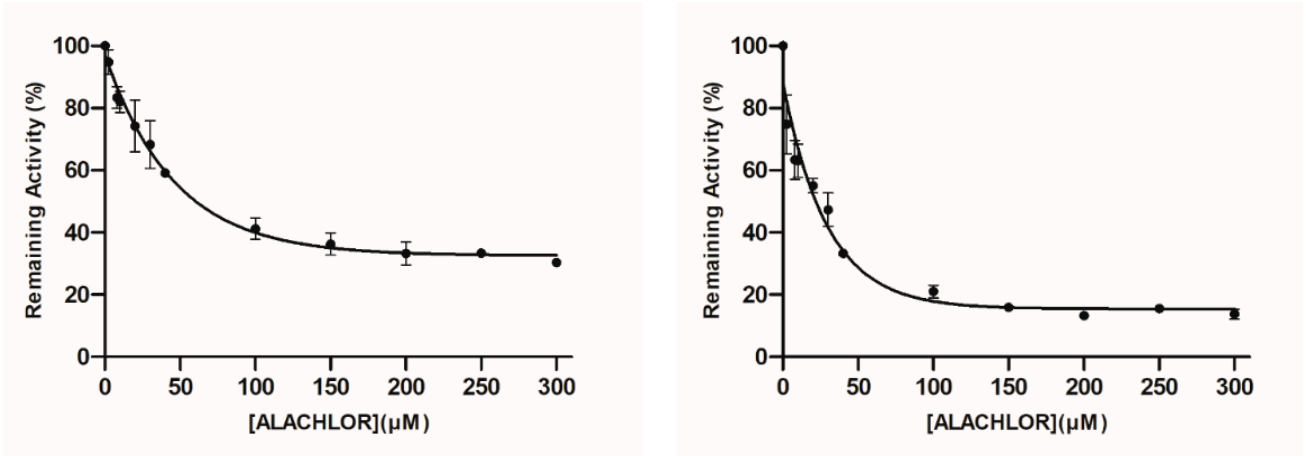

(**b**) (i) (ii)

Figure 3. (**a**) Lineweaver-Burk plots for the inhibition of *Gm*GSTU4-4 and *Gm*GSTsf by hAlachlor. (**i**) Inhibition of *Gm*GSTU4-4 by hAlachlor (0 µM (●), 0.04 mM (■), 0.08 mM (▼)) using constant concentration of GSH and the concentration of CDNB was varied. (**ii**) Inhibition of *Gm*GSTsf by hAlachlor (0 µM (●), 0.008 mM (■), 0.02 mM (▼)) using constant concentration of GSH and the concentration of CDNB was varied; (**b**) Dose-response curves for the inhibition of *Gm*GSTU4-4 (**i**) and *Gm*GSTsf (**ii**) by hAlachlor.

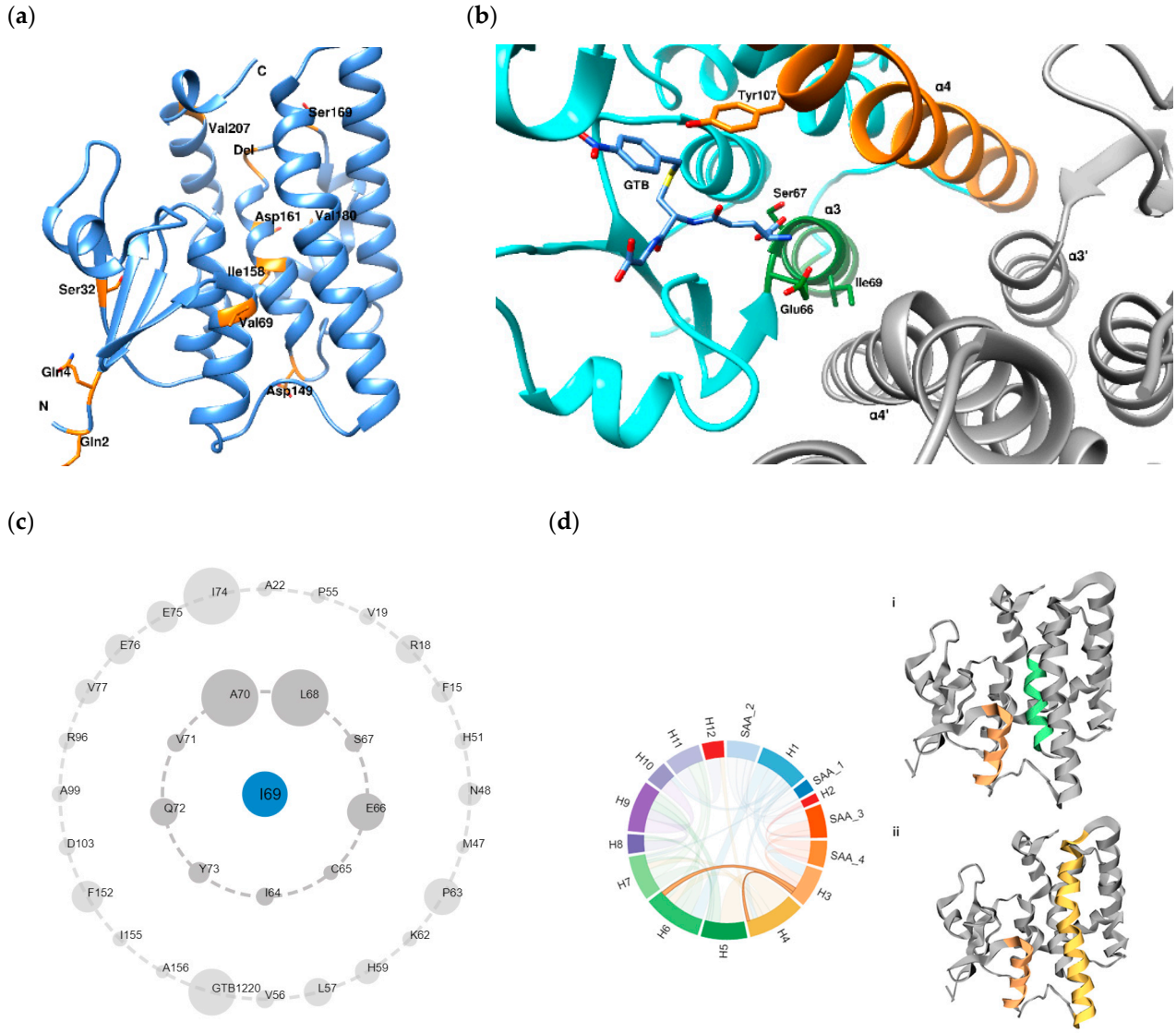

Figure 4. Structural analysis. (**a**) The predicted structure of *Gm*GSTsf. The mutated amino acid residues (Table 1) are shown as stick representations and labeled; (**b**) Interactions of Ile69 in the structure of *Gm*GSTU4-4 (PDB code: 2vo4). The bound inhibitor S-nitrobenzyl-glutathione (GTB) is shown as stick representation and colored according to the atom type. The amino acid residues Glu66 and Ser67 that contribute to the formation of the electron-sharing network are shown as stick representations and labeled. The second subunit in the dimer is coloured in grey; (**c**) Asteroid plot of interactions of Ile69 in the parent enzyme *Gm*GSTU4-4 (PDB code: 2vo4). The inner ring shows direct individual contacts and the outer ring indirect individual contacts. The size of each circle is proportional to the total number of contacts involved. The diagrams were created by Protein Contact Atlas [46]; (**d**) Chord plot of the interactions between helix α3 (brown) and helix α6 (i, green) or helix α4 (ii, yellow-brown).

Table 4. Comparison of non-covalent interactions involved with amino acid at position 69 in *Gm*GSTU4-4 (Ile69) and *Gm*GSTsf (Val69). The analysis was carried out using the Arpeggio web server [47].

Type of Interaction	*Gm*GSTU4-4	*Gm*GSTsf
Polar contacts	4	3
Weak polar contacts	3	2
Hydrogen bonds	2	2
Weak hydrogen bonds	4	2
Hydrophobic contacts	11	6

The monomers of the *Gm*GSTU4-4 form a two-fold symmetry. In each monomer, the N-terminal domain of the one subunit is in contact with the C-terminal domain of the second subunit, and vice versa. The loop α2-β2, the strand β3 and the helix α3 of the N-terminal domain interact with the helices α4 and α5 of the C-terminal domain. The helix α3 and α4 provides residues for the symmetric arrangement of the two subunits and form the lock-and-key motif. Besides, the amino acid at position 69 is part of the lock-and-key motif [38,49] that contributes to helix α4 stabilization and structural integrity. Worthy of note, helix α4 provides key amino acid residues, such as Tyr107 and Trp114, that affect product release and are the main determinants of both k_{cat} and k_{cat}/K_m regulation [40].

The electron-sharing network has been established to play an important role in the catalysis of GSTs. It allows the glutamyl γ-carboxylate of GSH to accept the H^+ from the sulfhydryl group of glutathione and function as a base [40,49,51]. A water molecule is involved in the transfer of the H^+ from the sulfhydryl group to the γ-glutamyl carboxylate, affecting the rate of catalysis. In the *Gm*GSTU4-4, the electron-sharing network is composed of the strictly conserved residues Arg18, Glu66, Ser67, and Asp103. We can speculate that conformation changes caused by the Ile69Val mutation may affect either the ionization of GSH or the rate of proton transfer from –SH to γ-glutamyl carboxylate, leading to enhanced reaction rate.

3.3. Enzyme Immobilization

The best suited enzyme for the development of an analytical biosensor should display high activity to place the threshold of sensitivity/detection as low as possible. Therefore, the improved catalytic and alachlor-binding capabilities of *Gm*GSTsf variant prompted us to exploit it for developing a GST biosensor for the direct monitoring of alachlor in water samples.

For the construction of the biosensor, the *Gm*GSTsf variant was immobilized directly on a polyvinylidenefluoride membrane by crosslinking with glutaraldehyde [16,52]. The functionalized membrane was placed on the inner surface of a plastic cuvette (Figure 5a). Glutaraldehyde was chosen as a cross-linking agent to generate a three-dimensional network consisting of *Gm*GSTsf interconnected through its exposed amino groups with bovine albumin (BSA). BSA was used to provide mechanical and physicochemical stabilization of the system. Figure 5b shows the reaction progress of the catalytic reactions (CDNB and alachlor as substrates) using the membrane-immobilized *Gm*GSTsf. The curves were obtained by measuring the rate of proton release (HCl) from the conjugation reactions (Scheme 1) using a pH electrode.

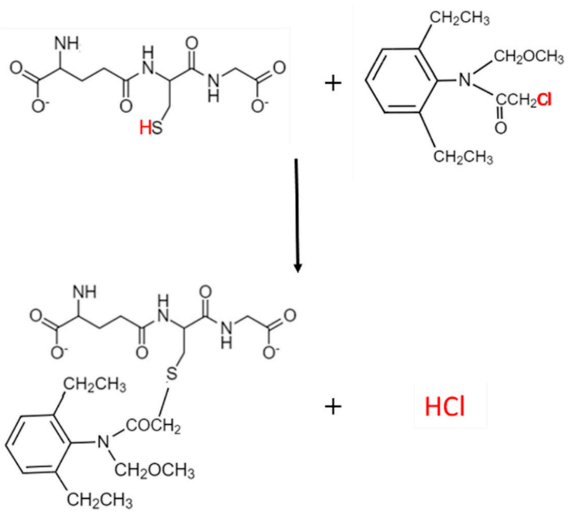

Scheme 1. The reaction between GSH and alachlor, catalyzed by *Gm*GSTsf.

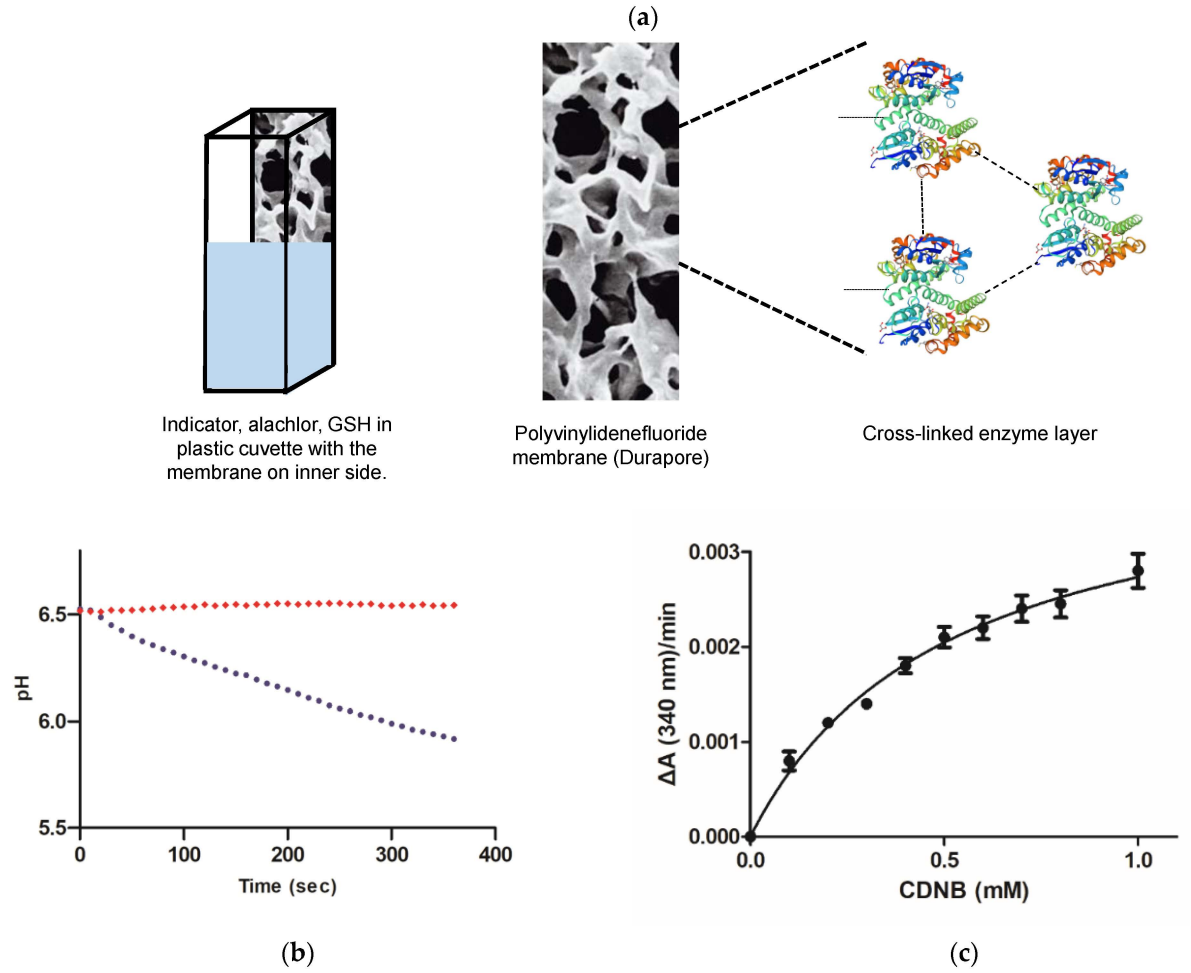

Figure 5. (**a**) Schematic diagram of the immobilization of the enzyme; (**b**) Reaction rate curves measured using a pH electrode. The reactions were carried out using immobilized *Gm*GSTsf using CDNB as substrate (●). Blank experiment (♦), without substrates; (**c**) Kinetic analysis of the immobilized *Gm*GSTsf enzyme for the CDNB/GSH conjugation reaction. The concentration of GSH was constant and the concentration of CDNB was varied. The CDNB/GSH conjugation reaction was monitored at 340 nm.

The immobilized enzyme was subjected to kinetics analysis to determine whether its kinetic properties were affected by the immobilization reaction. The results are shown in Figure 5c. The enzyme displayed a K_m 0.52 ± 0.0711 mM for CDNB, very close to that obtained with the free enzyme (Table 2), suggesting that the immobilized enzyme had retained its kinetic features.

3.4. Thermal Stability of the Immobilized Enzyme

To evaluate the storage stability of the immobilized enzyme, heat inactivation studies were accomplished (Figure 6). The immobilized enzyme, along with the free enzyme, was incubated at 4 °C in potassium phosphate buffer (1 mM, pH 7.5) and subsequently assayed for residual activity. The free enzyme was inactivated almost completely in 15 days at 4 °C. However, the immobilized enzyme exhibited significantly higher stability and lost less than 30% of its initial activity after 15 days of incubation. These findings indicate that the immobilization of *Gm*GSTsf on polyvinylidenefluoride membrane significantly improved the enzyme operational stability upon storage at 4 °C, an important consideration that determines the practical viability of the biosensor.

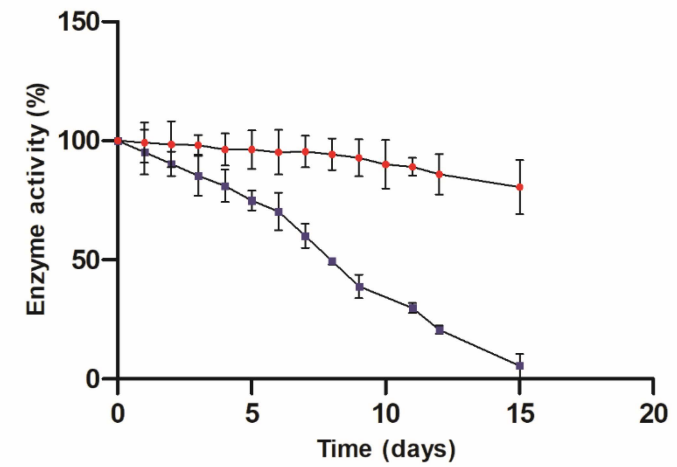

Figure 6. Stability analysis of the *Gm*GSTsf enzyme. Time course of inactivation of the free (■) and the immobilized *Gm*GSTsf enzyme (●) at 4 °C.

3.5. The Basis of an Optometric Biosensor for Alachlor Determination

The assay was based on the activity of *Gm*GSTsf to catalyze the reaction of GSH with alachlor with the simultaneous production of H^+. The amount of produced H^+ is proportional to the concentration of alachlor (Scheme 1). Therefore, the concentration of alachlor can be determined indirectly by colorimetric measurements of pH alterations in the presence of a pH indicator. The proposed optometric biosensor makes use of the chromogenic alterations of the bromocresol green in order to transduce the catalytic reaction into an optical signal. Optometric biosensors show several advantages compared to the common chromatographic methods, such as cost effectiveness, direct determination, and easy applicability in routine analysis [52,53].

Figure 7a shows typical spectra obtained during the reaction and Figure 7b illustrates the rate of absorbance changes at 620 nm. The slope was calculated for a 30 min reaction after initiation of the enzymatic reaction. The phosphate concentration in the buffer solution was 1 mM. Lower signals were obtained for higher buffer capacities, for a given substrate concentration; however, larger buffer concentrations (>2 mM) compromised sensor response. Figure 7c shows the calibration curve obtained using different concentrations of alachlor. It can be seen that the rate of absorbance change at 620 nm is linearly related to alachlor concentration within the concentration range of 0–300 μM.

Natural water samples were used for recovery experiments. The samples were spiked with known concentrations of alachlor and the amounts of alachlor were determined using the standard curve. The results are shown in Table 5 and Figure 7d. The study revealed that alachlor recoveries ranged between 92 and 112%, with mean value = 99.05 (N = 6), SD = 8.247 and Std. Error = 3.367. Correlation analysis between the added and found alachlor concentrations is shown in Figure 7d (R^2 0.9863, p = 0.0014).

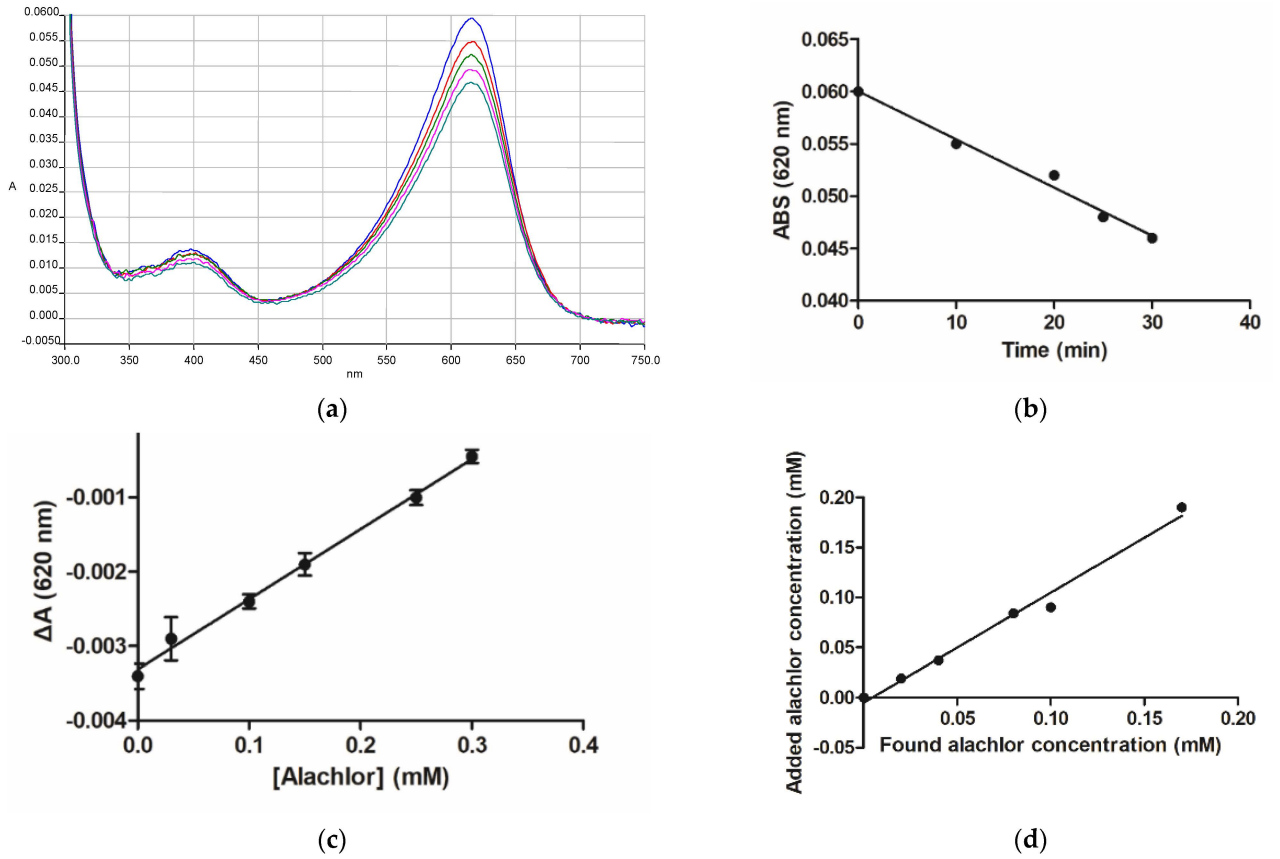

Figure 7. (**a**) Visible spectra of bromocresol green monitored after 0, 10, 20, and 30 min (from top to bottom) of enzymatic reaction; (**b**) Dependence of absorbance at 620 nm on time; (**c**) Calibration curve of the absorbance change at 620 nm on alachlor concentration (0–300 μM). The absorbance change at 620 nm was calculated as a difference between reference signal (control, spontaneous reaction in the absence of enzyme) and reaction signal; (**d**) Recovery experiments using natural water samples spiked with known amounts of alachlor. The concentrations of spiked alachlor (added alachlor) were calculated based on the standard curve (found alachlor).

Table 5. Recovery experiments using natural water samples. The concentrations of spiked alachlor were found using the standard curve.

Added Alachlor Concentrations (mM)	Found Alachlor Concentrations (mM)	%
0	0	100
0.02	0.019	95.0
0.04	0.037	92.5
0.08	0.084	105
0.10	0.09	90
0.17	0.19	111.8

4. Conclusions

In the present study we report on a protein engineering approach for the creation of a mutant glutathione transferase with improved catalytic performance toward the alachlor/GSH conjugation reaction. We showed that the symmetric structure of *Gm*GSTU4-4 can be efficiently manipulated through in vitro directed evolution, making new enzymes with altered catalytic activity and specificity. The engineered variant was exploited for the development of an optometric GST-based biosensor for alachlor determination in water samples. The advantages of this biosensor include low cost, real-time detection, and a wide linear range.

Author Contributions: Conceptualization, F.P., N.E.L.; formal analysis, F.P.; investigation, F.P., M.F.; writing—original draft preparation, M.F., A.C.P., N.E.L.; supervision, N.E.L.; All authors have read and agreed to the published version of the manuscript.

Funding: This research was co-financed by Greece and the European Union (European Social Fund-ESF) through the Operational Programme «Human Resources Development, Education and Lifelong Learning» in the context of the project "Reinforcement of Postdoctoral Researchers—2nd Cycle" (MIS-5033021), implemented by the State Scholarships Foundation (IKϒ).

Institutional Review Board Statement: Not applicable.

Informed Consent Statement: Not applicable.

Data Availability Statement: Data is contained within the article.

Acknowledgments: FP acknowledges the State Scholarships Foundation (IKϒ) for financial support. This research is co-financed by Greece and the European Union (European Social Fund- ESF) through the Operational Programme «Human Resources Development, Education and Lifelong Learning» in the context of the project "Reinforcement of Postdoctoral Researchers—2nd Cycle" (MIS-5033021), implemented by the State Scholarships Foundation (IKϒ). ACP thanks Biocenter Finland for infrastructure support.

Conflicts of Interest: The authors declare no conflict of interest. The funders had no role in the design of the study; in the collection, analyses, or interpretation of data; in the writing of the manuscript, or in the decision to publish the results.

References

1. Allocati, N.; Masulli, M.; Di Ilio, C.; Federici, L. Glutathione transferases: Substrates, inihibitors and pro-drugs in cancer and neurodegenerative diseases. *Oncogenesis* **2018**, *7*, 1–15. [CrossRef]
2. Mihaljević, I.; Bašica, B.; Maraković, N.; Kovačević, R.; Smital, T. Interaction of organotin compounds with three major glutathione S-transferases in zebrafish. *Toxicol. In Vitro* **2020**, *62*, 104713. [CrossRef] [PubMed]
3. Labrou, N.E.; Papageorgiou, A.C.; Pavli, O.; Flemetakis, E. Plant GSTome: Structure and functional role in xenome network and plant stress response. *Curr. Opin. Biotechnol.* **2015**, *32*, 186–194. [CrossRef]
4. Cummins, I.; Dixon, D.P.; Freitag-Pohl, S.; Skipsey, M.; Edwards, R. Multiple roles for plant glutathione transferases in xenobiotic detoxification. *Drug Metab. Rev.* **2011**, *43*, 266–280. [CrossRef] [PubMed]
5. Nianiou-Obeidat, I.; Madesis, P.; Kissoudis, C.; Voulgari, G.; Chronopoulou, E.; Tsaftaris, A.; Labrou, N.E. Plant glutathione transferase-mediated stress tolerance: Functions and biotechnological applications. *Plant Cell Rep.* **2017**, *36*, 791–805. [CrossRef] [PubMed]
6. Gullner, G.; Komives, T.; Király, L.; Schröder, P. Glutathione S-Transferase Enzymes in Plant-Pathogen Interactions. *Front. Plant Sci.* **2018**, *9*, 1836. [CrossRef]
7. Gallé, A.; Czékus, Z.; Bela, K.; Horváth, E.; Ördög, A.; Csiszár, J.; Poór, P. Plant Glutathione Transferases and Light. *Front. Plant Sci.* **2019**, *9*. [CrossRef]
8. Stavridou, E.; Michailidis, M.; Gedeon, S.; Ioakeim, A.; Kostas, S.; Chronopoulou, E.; Labrou, N.E.; Edwards, R.; Day, A.; Nianiou-Obeidat, I.; et al. Tolerance of Transplastomic Tobacco Plants Overexpressing a Theta Class Glutathione Transferase to Abiotic and Oxidative Stresses. *Front. Plant Sci.* **2019**, *9*, 1861. [CrossRef] [PubMed]
9. Dixon, D.P.; Edwards, R. Protein-Ligand Fishing in planta for Biologically Active Natural Products Using Glutathione Transferases. *Front. Plant Sci.* **2018**, *9*, 1659. [CrossRef]
10. Chronopoulou, E.; Kontouri, K.; Chantzikonstantinou, M.; Pouliou, F.; Perperopoulou, F.; Voulgari, G.; Bosmali, E.; Axarli, I.; Nianiou-Obeidat, I.; Madesis, P.; et al. Plant Glutathione Transferases: Structure, Antioxidant Catalytic Function and in planta Protective Role in Biotic and Abiotic Stress. *Curr. Chem. Biol.* **2015**, *8*, 58–75. [CrossRef]
11. Hodges, R.E.; Minich, D.M. Modulation of Metabolic Detoxification Pathways Using Foods and Food-Derived Components: A Scientific Review with Clinical Application. *J. Nutr. Metab.* **2015**, *2015*, 1–23. [CrossRef] [PubMed]
12. Mazari, A.M.; Mannervik, B. Drosophila GSTs display outstanding catalytic efficiencies with the environmental pollutants 2,4,6-trinitrotoluene and 2,4-dinitrotoluene. *Biochem. Biophys. Rep.* **2016**, *5*, 141–145. [CrossRef] [PubMed]
13. Ahmad, L.; Rylott, E.L.; Bruce, N.C.; Edwards, R.; Grogan, G. Structural evidence for Arabidopsis glutathione transferase AtGSTF2 functioning as a transporter of small organic ligands. *FEBS Open Bio* **2016**, *7*, 122–132. [CrossRef] [PubMed]
14. Sylvestre-Gonon, E.; Law, S.R.; Schwartz, M.; Robe, K.; Keech, O.; Didierjean, C.; Dubos, C.; Rouhier, N.; Hecker, A. Functional, Structural and Biochemical Features of Plant Serinyl-Glutathione Transferases. *Front. Plant Sci.* **2019**, *10*, 608. [CrossRef]
15. Perperopoulou, F.; Pouliou, F.; Labrou, N.E. Recent advances in protein engineering and biotechnological applications of glutathione transferases. *Crit. Rev. Biotechnol.* **2017**, *38*, 511–528. [CrossRef]
16. Andreou, V.G.; Clonis, Y.D. Novel fiber-optic biosensor based on immobilized glutathione S-transferase and sol–gel entrapped bromcresol green for the determination of atrazine. *Anal. Chim. Acta* **2002**, *460*, 151–161. [CrossRef]

17. Morou, E.; Ismail, H.M.; Dowd, A.J.; Hemingway, J.; Labrou, N.; Paine, M.J.I.; Vontas, J.; Labrou, N. A dehydrochlorinase-based pH change assay for determination of DDT in sprayed surfaces. *Anal. Biochem.* **2008**, *378*, 60–64. [CrossRef]
18. Kapoli, P.; Axarli, I.A.; Platis, D.; Fragoulaki, M.; Paine, M.; Hemingway, J.; Vontas, J.; Labrou, N.E. Engineering sensitive glutathione transferase for the detection of xenobiotics. *Biosens. Bioelectron.* **2008**, *24*, 498–503. [CrossRef]
19. Chronopoulou, E.G.; Papageorgiou, A.C.; Markoglou, A.; Labrou, N.E. Inhibition of human glutathione transferases by pesticides: Development of a simple analytical assay for the quantification of pesticides in water. *J. Mol. Catal. B Enzym.* **2012**, *81*, 43–51. [CrossRef]
20. Chronopoulou, E.G.; Ataya, F.; Labrou, N.E. A Microplate-based Platform with Immobilized Human Glutathione Transferase A1-1 for High-throughput Screening of Plant-origin Inhibitors. *Curr. Pharm. Biotechnol.* **2018**, *19*, 925–931. [CrossRef] [PubMed]
21. Oliveira, T.I.; Oliveira, M.; Viswanathan, S.; Barroso, M.F.; Barreiros, L.; Nunes, O.C.; Rodrigues, J.A.; De Lima-Neto, P.; Mazzetto, S.E.; Morais, S.; et al. Molinate quantification in environmental water by a glutathione-S-transferase based biosensor. *Talanta* **2013**, *106*, 249–254. [CrossRef] [PubMed]
22. Chronopoulou, E.G.; Papageorgiou, A.C.; Ataya, F.; Nianiou-Obeidat, I.; Madesis, P.; Labrou, N.E. Expanding the Plant GSTome Through Directed Evolution: DNA Shuffling for the Generation of New Synthetic Enzymes with Engineered Catalytic and Binding Properties. *Front. Plant Sci.* **2018**, *9*, 1737. [CrossRef] [PubMed]
23. Materon, E.M.; Huang, P.-J.J.; Wong, A.; Ferreira, A.A.P.; Sotomayor, M.D.P.T.; Liu, J. Glutathione-s-transferase modified electrodes for detecting anticancer drugs. *Biosens. Bioelectron.* **2014**, *58*, 232–236. [CrossRef]
24. Fintschenko, Y.; Krynitsky, A.J.; Wong, J.W. Emerging Pesticide Residue Issues and Analytical Approaches. *J. Agric. Food Chem.* **2010**, *58*, 5859–5861. [CrossRef]
25. Rane, R.V.; Ghodke, A.B.; Hoffmann, A.A.; Edwards, O.R.; Walsh, T.K.; Oakeshott, J.G. Detoxifying enzyme complements and host use phenotypes in 160 insect species. *Curr. Opin. Insect Sci.* **2019**, *31*, 131–138. [CrossRef]
26. Pavlidi, N.; Vontas, J.; Van Leeuwen, T. The role of glutathione S-transferases (GSTs) in insecticide resistance in crop pests and disease vectors. *Curr. Opin. Insect Sci.* **2018**, *27*, 97–102. [CrossRef] [PubMed]
27. Gomes, H.D.O.; Menezes, J.M.C.; da Costa, J.G.M.; Coutinho, H.D.M.; Teixeira, R.N.P.; Nascimento, R.F.D. A socio-environmental perspective on pesticide use and food production. *Ecotoxicol. Environ. Saf.* **2020**, *197*, 110627. [CrossRef]
28. Ambrus, A. International Harmonization of Food Safety Assessment of Pesticide Residues. *J. Agric. Food Chem.* **2015**, *64*, 21–29. [CrossRef]
29. Heckmann, C.M.; Paradisi, F. Looking Back: A Short History of the Discovery of Enzymes and How They Became Powerful Chemical Tools. *ChemCatChem* **2020**, *12*, 6082–6102. [CrossRef]
30. Rix, G.; Watkins-Dulaney, E.J.; Almhjell, P.J.; Boville, C.E.; Arnold, F.H.; Liu, C.C. Scalable continuous evolution for the generation of diverse enzyme variants encompassing promiscuous activities. *Nat. Commun.* **2020**, *11*, 5644. [CrossRef]
31. Asemoloye, M.D.; Marchisio, M.A.; Gupta, V.K.; Pecoraro, L. Genome-based engineering of ligninolytic enzymes in fungi. *Microb. Cell Factories* **2021**, *20*, 1–18. [CrossRef] [PubMed]
32. Jensen, E.D.; Ambri, F.; Bendtsen, M.B.; Javanpour, A.A.; Liu, C.C.; Jensen, M.K.; Keasling, J.D. Integrating continuous hypermutation with high-throughput screening for optimization of cis,cis -muconic acid production in yeast. *Microb. Biotechnol.* **2021**. [CrossRef]
33. Sánchez, A.; Vila, J.C.; Chang, C.-Y.; Diaz-Colunga, J.; Estrela, S.; Rebolleda-Gomez, M. Directed Evolution of Microbial Communities. *Annu. Rev. Biophys.* **2021**, *50*. [CrossRef]
34. Chesters, G.; Simsiman, G.V.; Levy, J.; Alhajjar, B.J.; Fathulla, R.N.; Harkin, J.M. Environmental Fate of Alachlor and Metolachlor. In *Reviews of Environmental Contamination and Toxicology*; Springer: New York, NY, USA, 1989; Volume 110, pp. 1–74. [CrossRef]
35. Heydens, W.F.; Wilson, A.G.; Kier, L.D.; Lau, H.; Thake, D.C.; Martens, M.A. An evaluation of the carcinogenic potential of the herbicide alachlor4 to man. *Hum. Exp. Toxicol.* **1999**, *18*, 363–391. [CrossRef]
36. Skopelitou, K.; Muleta, A.W.; Papageorgiou, A.C.; Chronopoulou, E.; Labrou, N.E. Catalytic features and crystal structure of a tau class glutathione transferase from Glycine max specifically upregulated in response to soybean mosaic virus infections. *Biochim. Biophys. Acta (BBA) Proteins Proteom.* **2015**, *1854*, 166–177. [CrossRef] [PubMed]
37. Skopelitou, K.; Muleta, A.W.; Papageorgiou, A.C.; Chronopoulou, E.G.; Pavli, O.; Flemetakis, E.; Skaracis, G.N.; Labrou, N.E. Characterization and functional analysis of a recombinant tau class glutathione transferase Gm GSTU2-2 from Glycine max. *Int. J. Biol. Macromol.* **2017**, *94*, 802–812. [CrossRef] [PubMed]
38. Axarli, I.; Dhavala, P.; Papageorgiou, A.C.; Labrou, N.E. Crystallographic and Functional Characterization of the Fluorodifen-inducible Glutathione Transferase from Glycine max Reveals an Active Site Topography Suited for Diphenylether Herbicides and a Novel L-site. *J. Mol. Biol.* **2009**, *385*, 984–1002. [CrossRef]
39. Stemmer, W.P. DNA shuffling by random fragmentation and reassembly: In vitro recombination for molecular evolution. *Proc. Natl. Acad. Sci. USA* **1994**, *91*, 10747–10751. [CrossRef] [PubMed]
40. Axarli, I.; Muleta, A.W.; Vlachakis, D.; Kossida, S.; Kotzia, G.A.; Maltezos, A.; Dhavala, P.; Papageorgiou, A.C.; Labrou, N.E. Directed evolution of Tau class glutathione transferases reveals a site that regulates catalytic efficiency and masks co-operativity. *Biochem. J.* **2016**, *473*, 559–570. [CrossRef] [PubMed]
41. Skopelitou, K.; Labrou, N.E. A new colorimetric assay for glutathione transferase-catalyzed halogen ion release for high-throughput screening. *Anal. Biochem.* **2010**, *405*, 201–206. [CrossRef]

42. Benkert, P.; Tosatto, S.C.E.; Schomburg, D. QMEAN: A comprehensive scoring function for model quality assessment. *Proteins Struct. Funct. Bioinform.* **2007**, *71*, 261–277. [CrossRef] [PubMed]
43. Studer, G.; Rempfer, C.; Waterhouse, A.M.; Gumienny, R.; Haas, J.; Schwede, T. QMEANDisCo—Distance constraints applied on model quality estimation. *Bioinformatics* **2019**, *36*, 1765–1771. [CrossRef] [PubMed]
44. Laskowski, R.A.; Rullmann, J.A.C.; MacArthur, M.W.; Kaptein, R.; Thornton, J.M. AQUA and PROCHECK-NMR: Programs for checking the quality of protein structures solved by NMR. *J. Biomol. NMR* **1996**, *8*, 477–486. [CrossRef]
45. Eisenberg, D.; Lüthy, R.; Bowie, J.U. [20] VERIFY3D: Assessment of protein models with three-dimensional profiles. In *Macromolecular Crystallography Part B*; Academic Press: Cambridge, MA, USA, 1997; Volume 277, pp. 396–404. [CrossRef]
46. Kayikci, M.; Venkatakrishnan, A.J.; Scott-Brown, J.; Ravarani, C.N.J.; Flock, T.; Babu, M.M. Visualization and analysis of non-covalent contacts using the Protein Contacts Atlas. *Nat. Struct. Mol. Biol.* **2018**, *25*, 185–194. [CrossRef]
47. Jubb, H.C.; Higueruelo, A.P.; Ochoa-Montaño, B.; Pitt, W.R.; Ascher, D.B.; Blundell, T.L. Arpeggio: A Web Server for Calculating and Visualising Interatomic Interactions in Protein Structures. *J. Mol. Biol.* **2017**, *429*, 365–371. [CrossRef]
48. Mcgonigle, B.; Keeler, S.J.; Lau, S.-M.C.; Koeppe, M.K.; O'Keefe, D.P. A Genomics Approach to the Comprehensive Analysis of the Glutathione S-Transferase Gene Family in Soybean and Maize. *Plant Physiol.* **2000**, *124*, 1105–1120. [CrossRef] [PubMed]
49. Axarli, I.; Georgiadou, C.; Dhavala, P.; Papageorgiou, A.C.; Labrou, N.E. Investigation of the role of conserved residues Ser13, Asn48 and Pro49 in the catalytic mechanism of the tau class glutathione transferase from Glycine max. *Biochim. Biophys. Acta (BBA) Proteins Proteom.* **2010**, *1804*, 662–667. [CrossRef] [PubMed]
50. Robert, X.; Gouet, P. Deciphering key features in protein structures with the new ENDscript server. *Nucl. Acids Res.* **2014**, *42*, W320–W324. [CrossRef]
51. Winayanuwattikun, P.; Ketterman, A.J. An Electron-sharing Network Involved in the Catalytic Mechanism Is Functionally Conserved in Different Glutathione Transferase Classes. *J. Biol. Chem.* **2005**, *280*, 31776–31782. [CrossRef] [PubMed]
52. Tran-Minh, C.; Mulchandani, A.; Rogers, K. Enzyme Biosensors Based on pH Electrodes. In *Enzyme and Microbial Sensors: Techniques and Protocols*; Humana Press: Totowa, NJ, USA, 1998; Chapter 2; pp. 15–22.
53. Mulchandani, A.; Chen, W.; Mulchandani, P.; Wang, J.; Rogers, K.R. Biosensors for direct determination of organophosphate pesticides. *Biosens. Bioelectron.* **2001**, *16*, 225–230. [CrossRef]